Antioxidants and Redox Signaling

DOI: 10.1089/ars.2017.7362

Nature of Article: Original research communication

Title: A novel mechanism for atherosclerotic calcification-potential resolution of the oxidation paradox.

Author(s): Aladdin Riad, MS*, Chandrakala Aluganti Narasimhulu, PhD.*, Pragney Deme, PhD,* and Sampath Parthasarathy, MBA., PhD. **

Affiliation (s): Burnett School of Biomedical Sciences, College of Medicine, University of Central Florida, Orlando, FL, USA, 32827.

*Equal contribution

Abbreviated title: Azelaic acid in atherosclerotic calcification

****Name and complete address of corresponding author**:

Sampath Parthasarathy, Ph.D., MBA.

Burnett School of Biomedical Sciences, College of Medicine,

University of Central Florida.

6900 Lake Nona Blvd., Orlando, FL 32827.

Tel: (407) 266-7121

Fax: (407) 266-7002

Email: spartha@ucf.edu

Total word count: 3,347

No. of color figures: 3

No. of grayscale figures: 4

No. of supplementary figures: 5

No. of supplementary tables:2

No. of references: 59

Key words: atherosclerosis, calcification, dicarboxylic acids, lipid peroxides**,** azelaic acid

Antioxidants and Redox Signaling
A novel mechanism for atherosclerotic calcification-potential resolution of the oxidation paradox. (DOI: 10.1089/ars.2017.7362)

Abstract

Aim: In this study, we tested the hypothesis that lipid peroxide-derived dicarboxylic acids, by virtue of their ability bind to calcium, might be involved in atherosclerotic calcification. We determined the ability of azelaic acid (AzA) to promote calcification in human aortic smooth muscle cells (HASMC), identified AzA in human calcified atherosclerotic lesions, and compared its levels with control and non-calcified atherosclerotic lesions.

Results: HASMCs efficiently converted 9-oxononanoic acid (ONA), a lipid peroxide derived monocarboxylic aldehyde, to AzA. *In vitro* incubations of AzA micelles with HASMC resulted in the formation of calcium deposits which contained AzA. LC-MS analysis of human control uninvolved artery, non-calcified, and calcified lesions showed significant increase of AzA in calcified lesions compared to non-calcified and control tissues. Calcified mouse atherosclerotic lesions also showed substantial presence of AzA in calcium complexes.

Innovation: This study identifies a dicarboxylic acid, AzA, as an integral part of the calcium complex. The study also demonstrates the conversion of a lipid peroxidation product, ONA as a potential source of AzA, and establishes the presence of AzA in calcified materials isolated from human and mouse lesions.

Conclusion: The presence of AzA as a calcium sequestering agent in atherosclerotic lesions might indicate, a) participation of oxidized-LDL (Ox-LDL) derived products in calcification, b) explain the potential correlation between calcification and overall plaque burden (as Ox-LDL has been suggested to be involved in atherogenesis), c) could contribute to plaque stabilization *via* its anti-inflammatory actions, and d) might explain why antioxidants failed to affect atherosclerosis in clinical studies.

Antioxidants and Redox Signaling
A novel mechanism for atherosclerotic calcification-potential resolution of the oxidation paradox. (DOI: 10.1089/ars.2017.7362)
This paper has been peer-reviewed and accepted for publication, but has yet to undergo copyediting and proof correction. The final published version may differ from this proof.

Introduction

It is currently believed that atherosclerosis progresses as early fatty streak lesions progress to raised complex lesions, involving smooth muscle cell proliferation, which may eventually become calcified (14, 48, 52). Calcification is a major independent predictor of cardiovascular morbidity and mortality (11, 36). Smooth muscle cells express bone differentiation markers such as alkaline phosphatase, which is suggested to provide phosphate for the formation of calcium phosphate (12). Accordingly, it is widely believed that calcium (Ca) in lesions might be present as calcium phosphate. Calcification is mainly identified by staining techniques such as von Kossa or alizarin red S staining, or by physical imaging techniques such as computerized tomography scan (CT-Scan) (8,24,35,42). While these techniques detect mineralized calcium, they do not indicate the chemical form in which calcium is deposited.

During the past three decades, the concept of oxidized low density lipoprotein (Ox-LDL) has emerged as a key player in the development of atherosclerosis. Overwhelming *in vitro* and *in vivo* evidence supports the hypothesis (5, 41, 54). The failure of human antioxidant trials, however, raised concerns about the validity of the hypothesis, at least in humans. Numerous review articles have appeared on the topic, including the suggestion that oxidative stress might be beneficial under certain circumstances (29, 38, 39, 55).

The breakdown of peroxidized lipids into aldehydes, both free and core aldehydes, have been well documented (27, 32, 59). Linoleic acid is the major polyunsaturated fatty acid (PUFA) of LDL, and the oxidation of linoleic acid generates toxic and reactive aldehydes (e.g 4-hydroxy nonenal (4-HNE) and 9-oxononanoic acid (ONA)) which have been shown to be highly pro-inflammatory (16, 22, 25, 43). However, aldehydes are also extremely oxidation-labile and are readily converted into carboxylic acids by a variety of enzymatic and non-enzymatic processes (20, 37). The Ox-LDL particle is also associated with the increased presence of Lyso phosphatidylcholine (Lyso-PtdCho) that could carry aldehydes and their oxidation products into cells (40, 44).

Antioxidants and Redox Signaling
A novel mechanism for atherosclerotic calcification-potential resolution of the oxidation paradox. (DOI: 10.1089/ars.2017.7362)

While 4-HNE has been well studied, aldehydes generated from the carboxylic acid end of fatty acid oxidation products, for example ONA, have not been studied as extensively. Its oxidation product, azelaic acid (AzA) is a poorly studied dicarboxylic acid (DCA). We recently reported that animals fed AzA had decreased atherosclerotic lesions as compared to control atherosclerotic mice (29).

Calcium phosphate as the sole calcified material does not explain the association of calcification with lipid-rich domains nor the latter's intra- and extra- cellular presence or its correlation with overall plaque burden (11). In this study, we considered the possibility that AzA or other DCAs, derived from lipid peroxide-derived aldehydes, by virtue of their ability to bind calcium might explain the relationship of calcification to the etiology (Ox-LDL) of atherosclerosis and the association with lipid accumulation. As a medium chain DCA, it would also bind calcium with higher affinity as compared to monocarboxylic acids (13, 18), and sequester calcium in lipid-rich domains. In addition, AzA has been noted to have anti-inflammatory properties and has been noted to decrease cytokine production by macrophages and inflammatory cells (3, 21). It also has been demonstrated to reduce oxidant production by leukocytes (15). Thus, AzA as a calcium binding lipid would explain the association of calcium with the lipid rich plaque and the association of calcification with products derived from Ox-LDL, and would account for the correlation of calcification with the overall plaque burden. This study is the first to suggest a direct link between DCA products derived from oxidation of aldehydes and calcification.

Using *in vitro* cultured human aortic smooth muscle cells (HASMC), we demonstrate the ability of ONA to get oxidized to AzA, and the ability of the latter to promote calcification in smooth muscle cells. We also unequivocally demonstrate the increased presence of AzA in calcified domains of atherosclerotic lesions by liquid chromatography-mass spectrometry (LC-MS) analysis, using both *in vitro* and *in vivo* (human and mice) samples.

Results:

Decomposition of lipid peroxides by HASMCs

Lipid peroxides and their aldehyde breakdown products play major roles in the progression of atherosclerosis. To demonstrate an active role of HASMCs in the decomposition of lipid

Antioxidants and Redox Signaling
A novel mechanism for atherosclerotic calcification-potential resolution of the oxidation paradox. (DOI: 10.1089/ars.2017.7362)

peroxides into aldehydes and to oxidize the latter into carboxylic acid, HASMCs were incubated with 100µM 13-hydroperoxyoctadecadienoic acid (HPODE), and increased AzA levels were observed by LC-MS analysis (Fig 1A). HPODE (Supplementary Fig.1) degradation was also monitored by the loss of leukomethylene blue (LMB) reactivity and the decrease in optical density at 234 nm (loss of conjugated dienes). As seen in the figure, the peroxides were lost in less than 2 hours in the presence of cells as compared to no cell incubations.

In addition, ^{14}C-HPODE was prepared and used further to confirm the HPODE decomposition in presence of HASMC for 6hours in HBSS. Autoradiography data indicated that HPODE was converted to AzA in the medium in presence of cells as compare to a no cell control, respectively (Supplementary Figure 2A).

Conversion of ONA to AzA in the presence of α-tocopherol and HASMC

Although AzA is present in many food materials in unknown quantities, in the body, it is likely to be generated from fatty acids. Oxidized fatty acids decompose to generate a number of different short chain (e.g. malondialdehyde, hexanal) to medium chain aldehydes (e.g. 4-HNE, ONA). Oxidation of these aldehydes, enzymatically or non-enzymatically, is expected to yield carboxylic acids. The oxidation of ONA is expected to yield AzA. To evaluate whether ONA is converted to AzA by cells, ONA was prepared and incubated with HASMCs as described in the methods, both in presence and absence of α-tocopherol. As shown in Figure 1B, LC-MS analysis showed a significant decrease in AzA at 6hrs of incubation with HASMCs in presence of α-tocopherol as compared to the absence of α-tocopherol, suggesting that antioxidants inhibit the conversion of ONA to AzA.

In addition, radioactive ^{14}C-ONA was also synthesized and used in these experiments. Autoradiography data showed a significant increase in AzA as shown in the figure (Supplementary Fig 2B) in the absence of α-tocopherol, whereas there was no or less change in ONA concentration as compared to control cell incubations at all time intervals.

Loading of HASMC with AzA results in calcification

To assess calcium accumulation upon AzA supplementation, HASMCs were treated with mixed micelles of Lyso-PtdCho/AzA as indicated in the methods section. At the concentrations used, little or no cytotoxicity was observed, as determined by microscopy and lactate dehydrogenase release. Percentage of cell viability was calculated using control

Antioxidants and Redox Signaling
A novel mechanism for atherosclerotic calcification-potential resolution of the oxidation paradox. (DOI: 10.1089/ars.2017.7362)
This paper has been peer-reviewed and accepted for publication, but has yet to undergo copyediting and proof correction. The final published version may differ from this proof.

untreated cells as 100% viability. As shown in the Supplementary Fig. 3, Lyso-PtdCho/AzA mixed micelles at the concentrations used have no obvious toxic effects on HASMCs, as compared to Lyso-PtdCho alone. After incubation and washings, the cells were stained with von Kossa stain, which stains calcium deposits by a dark brown/black silver residue. As seen in Fig. 2 there was minimal staining of control cells. Minimal staining was seen with Lyso-Ptdcho micelles alone. However, cells treated with the mixed micelles stained significantly darker which suggests robust calcification. β-glycerophosphate was used as a positive control. LC-MS analysis also confirmed the increased presence of AzA bound to calcium in HASMCs treated with Lyso-PtdCho/AzA mixed micelles, as shown in Figure 2F.

Detection of AzA in tissues

Calcification involves generation of insoluble complexes. In order to identify whether the mineralized calcium could contain AzA as a calcium complex, we first removed the non calcium-bound lipids by chloroform-methanol extraction, the soluble organic and aqueous phases were removed. This ensures that any non-calcium complexed AzA has been removed. The remaining insoluble material that contained protein and mineralized calcium complexes was subjected to acid hydrolysis with 10% acetic acid in methanol. The acid hydrolyzed material is expected to have calcium in the form of calcium chloride, and free AzA (no longer complexed with calcium). This was used to determine calcium and AzA concentrations. The tissue was processed as described in the methods.

Simply stated, this method first involved the removal of the non calcium complex lipids. After these non-mineralized lipids were removed, the calcified material was subjected to acid hydrolysis, which hydrolyzed the complex forming calcium chloride and free AzA. This free AzA was then extracted and quantified *via* LC-MS. This ensures any AzA analyzed was bound with calcium, as any free non-calcium complexed AzA would have been removed in the first lipid extraction.

Identification of calcification in aged ApoE-PON1 double knockout mice

ApoE-PON1 double knockout (DKO) mice of over 2 years of age on a normal diet were used, as this DKO mouse model has been shown to have increased atherosclerotic lesions (49). Comparatively, aged wild type mice and younger DKO mice (4 months) were used as controls. A significant increase in body weight, liver weight and plasma lipids were observed in the aged DKO mice as compared to controls (Supplementary Fig.4). These

Antioxidants and Redox Signaling
A novel mechanism for atherosclerotic calcification-potential resolution of the oxidation paradox. (DOI: 10.1089/ars.2017.7362)

mice also displayed extensive lesions upon dissection of the aortic arch, as indicated by the regions of white, opaque areas of the vessel (Fig. 3A). After confirming the presence of calcification by CT scan (Fig. 3B), histological examination of the aortic arch was performed and also displayed extensive calcification as determined by von Kossa (Fig. 3C) and alizarin red staining (Fig. 3D). Further, extensive calcification of the aortic arch and aortic root confirmed by the X-ray imaging (Fig. 3E-F). Figure 3G-I represents the phosphate, calcium, and AzA levels from pooled samples (n=9) in calcified and non-calcified lesions of mouse aortic samples. The results showed that AzA was found in significant amounts in calcified tissues as compared to non-calcified region. The lesion area of all the aortas as compared to control animals is represented in Supplementary Fig. 5.

Identification of calcification in human atherosclerotic aortic plaques

To identify the presence of AzA in calcified human atherosclerotic plaques we first needed to determine the presence of calcification in these human aortic samples by X-ray imaging (Fig. 4). Tissues were dissected to obtain non-lesion normal tissue, non-calcified atherosclerotic tissue, and calcified atherosclerotic lesions. Calcified domains were dissected from the non-calcified atherosclerotic plaques and re-imaged to verify dissection (Fig. 4A). Control tissue was also analyzed to confirm no calcification was present in the non-diseased tissue. The non-diseased and diseased pairs of aortic lesion tissue were acquired from the same individual, pathological reports of the tissues analyzed is shown in (Supplementary table 1). The tissues were used for the analysis of calcium, phosphate, and AzA levels. Fig. 4B–E represents the calcium, phosphate, and AzA levels in normal tissue, calcified lesions, and non-calcified lesions of human aortic samples. Quantification of calcium, phosphate, and AzA of individual samples were represented in Supplementary Table 2. MicroCT X-ray analysis of samples is also represented in the Fig. 5. As seen in the figure, presence of calcium was increased in calcified lesions as compared to other two controls. This confirmed the calcified lesions did indeed contain calcified deposits while the normal and non-calcified tissues were not calcified.

Antioxidants and Redox Signaling
A novel mechanism for atherosclerotic calcification-potential resolution of the oxidation paradox. (DOI: 10.1089/ars.2017.7362)
This paper has been peer-reviewed and accepted for publication, but has yet to undergo copyediting and proof correction. The final published version may differ from this proof.

AzA quantification in tissue samples

Human and mouse tissues were analyzed in a validated LC-MS method for quantitative analysis of AzA using AzA-D14 as an internal standard. The detected AzA presented in Supplementary Table 2 shows quantified AzA in nmoles. The representative LC-ESI-HRMS extracted ion chromatograms - AzA ($[M-H]^-$187.0976) and AzA-D14 (IS, ($[M-H]^-$ 201.1849)), ESI-MS and MS/MS spectra and proposed fragment ions shown in Fig. 6.

Increased presence of calcium and AzA in calcified human atherosclerotic lesions Calcium was identified in the control, non-calcified, and calcified lesions. As seen in Fig. 4, there was a several fold and significant increase in calcium in the calcified lesions, confirming the dissection and analytical techniques employed. The presence of AzA was established by LC/MS and we detected a significant increase in AzA concentrations in the calcified tissue as compared to the other two controls (Fig. 4). Although our focus was on AzA, oxidation of PUFA is expected to generate a plethora of DCAs, including a 12-carbon acid. We indeed observed several other minor mass ions in the isolated calcium complex, but have not established their chemical identities.

The amount of AzA, even if other DCAs (and even mono carboxylic acids) were present, did not fully match the levels of calcium. Combined with the unknown stoichiometry of the carboxylic acids with calcium, we kept in mind the possibility of the presence of free phosphates in the analysis. As seen in Fig. 4, although phosphates were present in significantly higher amounts in the calcium complex than azelate, the results of our study suggest that in addition to calcium phosphates, calcium azelate also contribute to atherosclerotic calcification.

Discussion

In this study, we present a new paradigm that atherosclerotic calcification may also involve calcium binding DCA products derived from Ox-LDL.

Calcium deposits are found more frequently and in greater amounts in elderly patients with atherosclerosis with more advanced lesions (7, 56). The extent of calcification has been correlated with plaque burden, suggesting that factors that contribute to atherosclerosis development may have a direct relationship with calcification.

Antioxidants and Redox Signaling
A novel mechanism for atherosclerotic calcification-potential resolution of the oxidation paradox. (DOI: 10.1089/ars.2017.7362)

The role of Ox-LDL and the effects of lipid peroxides and their aldehyde breakdown products on atherosclerosis have been studied extensively (46, 51). Aldehydes are chemically unstable intermediates and are readily oxidized to carboxylic acids, In addition to spontaneous oxidation, a variety of enzymes and processes are capable of converting aldehydes into carboxylic acids. In some cases (i.e. xanthine/aldehyde oxidases), the process itself generates free radicals (17, 28). We recently reported the oxidation of aldehydes by the myeloperoxidase (MPO) / HOCl system (45). Of particular interest to us is aldehyde oxidase 1 (AOX1), which has been reported as an ATP binding cassette transporter-A1 (ABCA1)-interacting protein (50). Most carboxylic acids derived from the oxidation of aldehydes formed via the decomposition of lipid peroxides are simple, short chain molecules from the ω-end. These are very rapidly metabolized by simple β-oxidation pathways and are rarely used as an anabolic intermediate. The DCA could be from the middle of the molecule (e.g. malondialdehyde) or mostly from the carboxyl end (e.g. AzA). Obviously some type of esterase/PLA2 is needed to release the carboxyl moiety.

In this study, we demonstrate that AzA may play a role in calcification. AzA is used extensively as an anti-inflammatory and antioxidant agent (19), but has not been implicated in atherosclerotic calcification. AzA has the ability to bind calcium forming a complex, and our *in vitro* studies have shown its ability to induce calcification of HASMC upon intracellular micelle delivery. In order to understand its involvement *in vivo*, we extracted calcified material from atherosclerotic plaques and were able to identify AzA upon acid hydrolysis of the insoluble calcified deposits. The LC-MS identification of AzA, both in mice and human lesions, in isolated mineralized calcium deposits, conclusively demonstrates that AzA was an integral part of the calcium deposits. Free AzA would have been removed by extraction with the organic solvent during lipid extraction and any soluble Ca salts would have been partitioned into the aqueous phase. Thus, the presence of both Ca and AzA in the insoluble material and their release only upon acid hydrolysis suggests that they are present together. This is the first study to detect medium chain DCA in the *calcium deposits* of human atherosclerotic lesions.

Ox-LDL is intimately involved in atherosclerotic progression, as it is internalized by macrophages during the formation of early atherosclerotic fatty streak lesions. Ox-LDL also plays a role in subsequent development of advanced lesions by promoting SMC migration

Antioxidants and Redox Signaling
A novel mechanism for atherosclerotic calcification-potential resolution of the oxidation paradox. (DOI: 10.1089/ars.2017.7362)
This paper has been peer-reviewed and accepted for publication, but has yet to undergo copyediting and proof correction. The final published version may differ from this proof.

and affecting plaque vulnerability. Thus, the presence of oxidized lipids, and products derived from oxidized lipids, would be expected to correlate with the overall plaque burden. As the current study implicates DCAs, including AzA in calcification, it would be no surprise that the extent of calcification is a representation of the overall plaque burden. Moreover, oxidized medium chain DCAs such as AzA are lipophilic, derived from lipids, and thus are expected to be present in the lipid rich domain of the lesion, where they may bind to calcium and form insoluble complexes.

There has been a great deal of debate about the role of calcification in plaque rupture (1, 23, 31, 34). Calcification has been noted as both intra- and extra- cellular deposits (53), the latter predominantly is associated with extracellular lipids. Many researchers believe that coronary arterial calcification may represent an attempt to protect the weakened atherosclerotic plaque prone to rupture (1, 57). Calcified lesions and fibrotic lesions are much stiffer than cellular lesions and are unlikely to be associated with sites of plaque rupture (1, 57). In fact, a recent study showed that less than 15% of the ruptured human lesions showed evidence of associated calcification (58). It is speculated that the plaque rupture often occurs at the interface between a calcified and non-calcified atherosclerotic area of the lesion. Thus, calcification could be seen as a potential stabilizing force that may increase the biochemical stability of the plaque by imparting rigidity while at the same time decreasing the plaque's mechanical stability. While the presence of calcium phosphate is not ruled out in this study, the finding that AzA, an anti-inflammatory molecule, is associated with calcium could suggest it imparts other potential effects to the calcified domain besides affecting the stability of calcified plaques.

Although the current studies provide support to the hypothesis that AzA might contribute to aortic calcification, additional proof is needed to suggest inhibition of AzA synthesis might lead to reduction of aortic calcification. Current limitations are: A) Laboratory mice require a longer period (over 18 months) to develop calcification. At this point, technology does not exist to demonstrate the presence of AzA *in vivo* or to detect/quantify calcification in vivo in live mice. B) While the current studies demonstrate Vit E or α-tocopherol could inhibit conversion of aldehydes to carboxylic acids, it's also known that α-tocopherol inhibits atherosclerosis in animal studies which might lead to inconclusive evidence as both atherosclerosis and lipid peroxidation will be inhibited. C) Dosage of

Antioxidants and Redox Signaling
A novel mechanism for atherosclerotic calcification-potential resolution of the oxidation paradox. (DOI: 10.1089/ars.2017.7362)

antioxidants or any specific inhibitors needed to inhibit this ONA to AzA conversion *in vivo* cannot be speculated at this point. Such studies might be of interest, but currently it's beyond the scope of the present study. D) There are numerous enzymatic pathways (xanthine oxidase, various isoforms of aldehyde dehydrogenases and aldehyde oxidases) that could oxidize ONA to AzA. It is nearly impossible to find common inhibitors that could be administered for a long time to prevent AzA formation *in vivo.*

Yet another limitation of the study is that the potential role of AzA in promoting calcification could only be deduced from data on current calcified deposits. On the other hand, the current study demonstrates the presence of AzA in association with mineralized calcium deposits. Whether the presence of AzA promotes calcification could only be surmised from its presence in the calcified regions of tissue samples, however, to establish the specific role of AzA in calcification is beyond the scope of the study as it requires longitudinal human studies.

Our findings are of great interest and could explain the failure of antioxidant trials in treating human atherosclerosis. Antioxidants inhibit a variety of oxidative processes, including many enzymatic and non-enzymatic oxidative pathways. We have noted the inhibition of conversion of ONA to AzA in the presence of antioxidants (Figure 1B). Thus, the formation of DCA from ONA may represent a protective mechanism to thwart plaque vulnerability. Furthermore, antioxidants under such circumstances might result in the accumulation of toxic and pro-inflammatory aldehydes and promote plaque vulnerability (Figure 7 - Scheme). Combined with our findings (29) that AzA prevented atherosclerosis without affecting lipid levels and decreased CD68 positive macrophages in the lesions, this study suggests additional benefits in promoting the oxidation of toxic aldehydes to innocuous carboxylic acids.

Innovation

Atherosclerosis has been suggested to involve the oxidation of LDL associated polyunsaturated fatty acids. Many aldehydes are formed as a result of decomposition of lipid peroxides. However, their propensity to undergo further oxidation to carboxylic acid has been vastly ignored. This is the first study to demonstrate the ability of AzA to bind calcium and suggest that calcium azealate could contribute to atherosclerotic calcification.

The presence of AzA in lesions might suggest why antioxidant trials might have failed to prevent atherosclerosis, as they would also inhibit the conversion of toxic aldehydes to carboxylic acids.

Methods

Materials and reagents

Reagents and chemicals were purchased from Sigma (St. Louis, MO). Declassified human atherosclerotic tissue samples were purchased from Collaborative Human Tissue Network (CHTN) from Ohio State University. All studies were performed following approval provided by the Institutional Review Board (IRB) of the University of Central Florida.

Cell culture

Human Aortic Smooth Muscle Cells (purchased from ATCC) were cultured in DMEM/F12 supplemented with 10% fetal bovine serum (FBS).

Preparation of HPODE

13-hydroperoxylinoleic acid (13-HPODE- 200 µmoles/L) was prepared as described previously (47). Lipid peroxide generated in the reaction system was analyzed by LMB assay (4), and the amount of peroxide generated was quantitated. The oxidized fatty acid was extracted with BHT free ether, dried under the stream of nitrogen, and stored at −20°C.

Similarly 200 µmoles/L radioactive ^{14}C-HPODE 1000 DPM/nmol, was prepared and used for the experiments.

Synthesis of 9-Oxononanoic Acid

9-Oxononanoic acid was prepared from oleic acid *via* erythro-9,10- dihydroxysteric acid (DHSA) (26, 30). Briefly, oleic acid was oxidized to dihydroxystearic acid using potassium permanganate and was oxidized further by sodium periodate to 9-ONA. After the reaction was completed, centrifugation was performed at 400g for 5min at 4°C to obtain clear supernatant. Supernatant was dried under the stream of nitrogen and purified by TLC using a solvent system of chloroform, tetrahydrofuran and acetic acid (30/3.3/0.1/6) and confirmed by 2,4-Dinitrophenylhydrazine (DNP) staining. Quality of the ONA was further confirmed by LC-MS analysis. For cell culture studies ONA was suspended in chloroform, dried under the stream of nitrogen and reconstituted with ethanol, further diluted with

Antioxidants and Redox Signaling
A novel mechanism for atherosclerotic calcification-potential resolution of the oxidation paradox. (DOI: 10.1089/ars.2017.7362)
This paper has been peer-reviewed and accepted for publication, but has yet to undergo copyediting and proof correction. The final published version may differ from this proof.

PBS and used as needed. Similarly radioactive ONA (1000 DPM/nmol) was synthesized from ^{14}C-oleic acid and used for the experiments. Standard AzA on TLC was confirmed by bromocresol green staining.

Treatment of cells with HPODE/ONA

HASMC were seeded at an initial density of 2 ×10^4. After attaining the confluency, cells were starved in serum free medium for 3hrs prior the treatments. Cells were treated with 100nmoles HPODE and 100nmoles of ONA for 4hrs in HBSS in presence and absence of 50µmoles/L α-tocopherol. After 4hrs of incubation intra- and extra-cellular levels of decomposition products were analyzed by LC-MS.

LC-MS analysis for *in vitro* cell culture experiments

Samples were analyzed by LC-MS as described in methodology section. Samples were extracted from cell lysate by 1 mL of methanol, pipetted well up and down about 5 times. The sample was centrifuged at 12000 rpm for 15 min. supernatant was collected and 5 µL of sample was injected for LC-MS analysis.

Thin layer chromatography and autoradiography ^{14}C-HPODE / ^{14}C-ONA

After treatment of cells with HPODE and ONA in presence and absence of α-tocopherol the cell culture medium and cellular lipid extracts were dissolved in 20 µl of chloroform and loaded on Silica Gel G TLC plate (Sigma, St. Louis, MO) with standards. Chloroform:Tetrahydrofuran:Acetic acid (90 : 10 : 0.5) was used as solvent system. After the separation, the TLC plate was left in the chemical hood for 10 minutes to let solvents evaporate. The dried TLC plate was covered with saran wrap and exposed to storage Phosphor screen (Perkin Elmer, MultiSensitive Storage Screen) for up to 48 hours. Autoradiography was performed by Cyclone Plus (Perkin Elmer Storage Phosphor System).

Micelle preparation

Azelaic acid (final concentration 100 µmole/L) was mixed with Lyso-PtdCho (final concentration 50 µmoles/L), vortexed vigorously, and dried under a nitrogen stream. The dried mixture was resuspended in 10mL of aqueous media, generating Lyso-PtdCho/AzA micelles, which were used for cell treatment every alternate day. 10mmoles/L β-glycerophosphate was used as a positive control.

Antioxidants and Redox Signaling
A novel mechanism for atherosclerotic calcification-potential resolution of the oxidation paradox. (DOI: 10.1089/ars.2017.7362)

WST-1 cell viability assay

The effect of the Lyso-PtdCho and mixed micelles on cell viability was determined by WST-1 assay (Roche Applied Science, IN). HASMC cells ($2.5x10^3$ cells/100 µL) were seeded in a 96-well plate and incubated overnight at 37°C in the presence of 5% CO_2. Medium was replaced with fresh medium containing 50µmoles/L Lyso-PtdCho, 50µmoles/L/100µmoles/L Lyso-PtdCho/AzA micelles. After incubation, 10µL of WST-1 reagent, (which is processed to formazan by cellular enzymes) was added to each well in 100µL of cell culture medium. Cells were further incubated for 4h at 37°C. Cell viability was determined by measuring absorbance at 450nm (630nm was used as reference wavelength) using a 96-well plate reader (Benchmark Plus Microplate Spectrophotometer System, Bio-Rad, Hercules, CA).

Induction of calcification in HASMCs by AzA

HASMCs were grown in standard growth medium supplemented with either Lyso-PtdCho (50µmoles/L) alone, or with 50µmoles/L/100µmoles/L Lyso-PtdCho/AzA micelles, or with sodium azelate (100µmoles/L) for 9 days. As a positive control for calcification, HASMCs were treated with 10 millimoles/L β-glycerophosphate. Calcification was detected by staining with Alizarin Red S and von Kossa staining.

Alizarin Red S staining

Tissue sections were washed with PBS twice, followed by two washes with deionized water, then stained with freshly prepared and filtered 2% Alizarin Red S (pH 4.2) reagent for 1 minute with gentle agitation. Alizarin Red S reagent was removed followed by two washes with deionized water and PBS, then imaged using the light microscope with the Leica DFC295 camera (Leica Camera AG, Solms, Germany). Calcium deposits were visualized by their red color.

Von Kossa staining

After micelle treatment, cells were washed four times with PBS and fixed in 10% formalin for 30 minutes on ice. Formalin was aspirated and cells were washed three times with PBS, followed by four washes with deionized water, then incubated with 1% silver nitrate for 4 hours (2 hours under an ultraviolet light followed by 2 hours under a bright fluorescent light). Following staining, silver nitrate solution was aspirated and the cells were washed with deionized water once. To remove background and nonspecific deposits, cells were

incubated with 5% sodium thiosulfate solution for 2 minutes, followed by washing twice with deionized water. Slides were mounted and imaged using the light microscope Leica DFC295 camera (Leica Camera AG, Solms, Germany). Calcium deposits are visualized as dark brown to black spots. Tissue sections were similarly stained.

Animals

ApoE-PON1 double knockout mice were developed using PON1$^{(-/-)}$ and ApoE$^{(-/-)}$ mice of C57BL/6J background from Jackson Laboratories (Bar Harbor, ME). Double knockouts were developed by crossing ApoE$^{(-/-)}$ mice with PON1$^{(-/-)}$ mice for 12 generations, as described by (49). The mice were genotyped by polymerase chain reaction (PCR) analysis of tail tip DNA, isolated according to the manufacturer's instructions using the Dneasy Blood and tissue DNA kit (Qiagen, Germantown, MD) followed by agarose gel electrophoresis. Specific primer sequences from Jackson Laboratory were used for synthesis and analysis of knockouts.

Twenty, over 2yr old mice weighing 30-35 g and 10 younger 4months old mice weighing 18-22gms male ApoE-PON1 DKO mice were used. Ten, seven month old C57BL6/J male mice were purchased and maintained. The animals were regularly monitored and a weekly record of body weight was maintained until used for experiments. All procedures were performed according to protocol approved by The Institutional Animal Care and Use Committee.

Collection of plasma and organs

After 2 years of age, mice were fasted overnight and anesthetized with 1-2% isoflurane. Fasting blood samples were collected into EDTA tubes by heart puncture. Plasma was separated as described previously (39) and stored at -80°C.

Isolation and quantification of mice aortic lesions

Isolation of the aorta and quantification of aortic lesions was performed as described previously (6, 9, 10). Lesion areas were marked on photographs. The lesion area was quantified using ImageJ software (2). Calcified lesions in aortas were analyzed by x-ray using the Xtreme imaging system. For histological analysis aortic roots were frozen immediately after imaging, cryosectioned, fixed, and used for Alizarin Red S staining and

Antioxidants and Redox Signaling
A novel mechanism for atherosclerotic calcification-potential resolution of the oxidation paradox. (DOI: 10.1089/ars.2017.7362)

von Kossa staining to determine the presence of calcium, as mentioned previously. All stained sections were observed under light microscope using Leica DFC295 camera (Leica Camera AG, Solms, Germany).

X-Ray analysis

Human and mouse aortic tissue samples were separated into calcified and non-calcified domains using the Bruker in-vivo Xtreme imaging system (Billerica, MA) and analyzed using the Bruker Molecular Imaging Software. X-ray analysis was conducted using an exposure time of 1.20 seconds.

Isolation calcified and non-calcified regions of the human aortic tissues

Following IRB approval control and Human calcified tissue samples were collected from Collaborative human tissue network (CHTN). 9-11 pairs of samples were used for the current study. The same tissue provided un-involved control, non-calcified, and calcified samples. Age, gender, pathology and disease severities of subjects are mentioned in supplementary table 1. Calcified tissues were imaged by using the Xtreme imaging machine. Non calcified and calcified tissues were separated and confirmed by X-ray analysis.

Micro CT analysis

To study the differences in the calcified and non-calcified human atherosclerotic plaques µCT analysis was performed by using the Quantum FX µCT scanner (PerkinElmer, Waltham, MA) with the following settings: isotropic voxel size of 10 µm, 70 kV, 160 mA, 5 mm field of view, 3 min scan (FINE setting) per sample. Raw µCT images were processed using Quantum FX µCT software (PerkinElmer). For the analysis of calcified tissue, the volume enclosing the entire 6-cm aorta segment is selected. Images were segmented into calcified and non-calcified tissue on each volume of interest using a global threshold method. After calibration and identification of calcified tissue, the amount of calcium in the sample were quantified using the Quantum FX µCT Software.

Aortic tissue sample preparation for LC-MS analysis

Tissue (300 mg for human and 50 mg for mice) was weighed and lyophilized to complete dryness. Dried tissue samples of human (50 mg) and mice (10 mg) were taken for analysis. The sample extraction procedure involved two steps. First, lipids and material not associated with calcium domain were removed as follows: tissue samples were

homogenized and extracted sequentially, with 6 mL of chloroform and then 6 mL of methanol. Samples were vortexed well and centrifuged at 2500 rpm for 20 min. The supernatants were removed. Second, for extraction of organic acids associated with calcium, the precipitation was incubated in methanol (6 mL × 2) containing 10% acetic acid (HAc) at 45°C for 45 min, vortexed well, centrifuged at 2500 rpm and the supernatants were collected. Two extracts were combined and evaporated to dryness under the gentle stream of nitrogen. The residues were dissolved in 500 µL of methanol containing 0.1% formic acid. The samples were centrifuged at 12000 rpm for 20 min and filtered through 0.22 µm PVDF syringe filters (Fisher Scientific, # 0992728A) for LC-MS/MS analysis. For calcium and phosphate detection, samples were incubated in water containing 10% HAc at 50°C for 1 hr, after the removal of lipids and materials that are not associated with calcium.

LC-MS analysis

Samples were analyzed on Agilent 1200 series high performance liquid chromatography (HPLC) (Agilent Technologies, CA, USA). The HPLC system consisted of G1379B degasser, G1311A quaternary pump, HTC PAL autosampler and G1316A column compartment coupled to 6520B hybrid quadrupole time-of-flight mass spectrometer (QTOF-MS) equipped with dual electrospray ionization (ESI) source. Analytes were separated on PerkinElmer Brownlee SPP C18 (100 × 2.1 mm, L×ID, 2.7 µm PS, #N9308404) UHPLC column protected with C18 (5×2.1 mm, L×ID, 2.7 µm PS, # N9308513) guard column. Binary mobile phase gradient program was used to separate the molecules, pump-A: methanol and pump-B: water, both containing 0.1% (v/v) formic acid. The linear gradient program was as follows: 0–8 min, 90% B; 8–25 min, 10% B; 25–38 min, 10% B; 38-38.1; 90% B; 38.1–45 min 90% B. The column was operated at 45°C with a constant mobile phase flow rate of 0.3 mL/min.

Data were acquired in ESI negative mode for identification of organic acids associated with calcified domains. Mass spectral data were collected in the mass range of 20–1700 m/z, in auto MS/MS mode to obtain MS and MS/MS data simultaneously. The mass spectrometer was tuned at 4GHz high resolution mode at low 1700 m/z range with a manufacturer ESI-TOF calibration solution (Agilent, #G1969-85000). To ensure good mass accuracy TOF reference mass solution (Agilent, #G1969-85001) was continuously introduced via the

second nebulizer throughout the analysis. ESI source parameters were optimized and operated under the following conditions: capillary voltage: 3.5 kV; source temperature: 320°C; nitrogen (N_2) used as a drying and nebulizer gas: 12 L/min and 50 psig respectively, TOF parameters: Fragmentor and skimmer voltages: 100 V and 65 V respectively. N_2 used as a CID gas for MS/MS studies, optimized collision energy (CE) set at 22 volts. The MS data were collected and processed using masshunter qualitative analysis version B.07.00 software.

The presence of AzA was confirmed by its high resolution mass detected as deprotonated molecular ion at *m/z* 187.0987 eluted at 16.95 (± 0.2). Also confirmed further by analyzing authentic reference standard of AzA and MS/MS fragmentation spectral match with the reference standard.

Quantification of AzA

The developed LC-MS method was validated according to the FDA guidelines (Bioanalytical method validation, guidance for Industry) for quantitative analysis of AzA in three types of tissue samples (normal, diseased non-calcified and calcified tissues). Limit of detection (LOD) and limit of quantifications (LOQ) were calculated in terms of signal to noise ratio (LOD, S/N≥3 and LOQ, S/N≥ 10), were found to be 50 and 75 pmoles respectively. The linearity of AzA is examined in matrix spiked and in neat solvent spiked samples at the concentration range of 75 to 5000 pmoles, using stable labeled isotope AzA-D14 as an internal standard (IS) at a constant concentration of 250 pmoles. The calibration curves were graphed between the area under the curve ratio of AzA/AzA-D14 against the concentration of AzA. The matrix spiked and neat solvent calibration curves of AzA shown to be linear, with regression coefficients (R^2) greater than 0.995. Quality control sample were analyzed in triplicates (n=3) at three different concentrations 75, 150 and 300 pmoles to evaluate precision of the method in terms relative standard deviations (% RSD), observed to be below 13%.

Antioxidants and Redox Signaling
A novel mechanism for atherosclerotic calcification-potential resolution of the oxidation paradox. (DOI: 10.1089/ars.2017.7362)
This paper has been peer-reviewed and accepted for publication, but has yet to undergo copyediting and proof correction. The final published version may differ from this proof.

Antioxidants and Redox Signaling
A novel mechanism for atherosclerotic calcification-potential resolution of the oxidation paradox. (DOI: 10.1089/ars.2017.7362)

Matrix effect of tissue samples

Matrix effect (ME, %) of the method was determined by comparing response ratio of analyte and IS (AzA/AzA-D14, AUC) in standard solution against with the matrix spiked standards (33). ME was calculated at three different concentration levels, 75 (LOQ), 150 and 300 pmoles, in triplicates (n=3) and found to be 10.13, 8.63 and 5.6 % respectively.

Extraction recovery of AzA from tissues samples

Extraction recovery (ER, %) of AzA was calculated by pre extraction and post extraction spikes of calcium-azelate (Ca-AzA). Blank matrix ensured that AzA was absent in tissue extract/diluted matrix for matrix spiking experiments. Pre extraction spike: Ca-AzA added to the tissue samples and stored at -80°C overnight, thawed the next day, homogenized and extracted as described in sample preparation section. post extraction spike: Ca-AzA was added to the acidified methanol tissue extract and incubated at 45°C for 30 min. ER carried out at three different concentrations, 75 (LOQ), 150 and 300 pmoles in triplicates (n=3) and found to be 71.7, 76.7 and 81.2 % respectively.

Calcium and Phosphate quantification

Samples were prepared as described in methods; calcium and phosphate were quantified using Abcam (Cambridge, MA) colorimetric assay kits, calcium colorimetric assay (ab102505) and phosphate colorimetric assay (ab65622) following the instructions of supplier's protocol.

Statistical analysis

Values are presented as a mean ±standard deviation (SD), and statistical analyses were performed by using student's t-test, with $P<0.05$ as the level of significance. For multiple group comparisons, one way ANOVA-Bonferroni multiple comparison test was used with $p<0.05$ as the level of significance.

Acknowledgement: This study was supported by NIH R01HL123283-01 (Parthasarathy) grant on "Role of aldehyde oxidation in atherosclerosis."

Disclosures: The authors do not have financial interests or conflicts.

Antioxidants and Redox Signaling
A novel mechanism for atherosclerotic calcification-potential resolution of the oxidation paradox. (DOI: 10.1089/ars.2017.7362)

References

1 Abedin M, Tintut Y, and Demer LL. Vascular calcification: mechanisms and clinical ramifications. *Arterioscler. Thromb. Vasc. Biol*. 24:1161–1170, 2004.

2 Abramoff MD, Magelhaes PJ, and Ram SJ: Image Processing with ImageJ. *Biophotonics Int* 11:36–42, 2004.

3 Akamatsu H, Komura J, Asada Y, Miyachi Y, and Niwa Y. Inhibitory effect of azelaic acid on neutrophil functions: a possible cause for its efficacy in treating pathogenetically unrelated diseases. *Arch. Dermatol. Res* 283:162–166, 1991.

4 Auerbach BJ, Kiely JS, and Cornicelli JA. A spectrophotometric microtiter-based assay for the detection of hydroperoxy derivatives of linoleic acid. *Anal Biochem* 201: 375–380, 1992

5 Berliner J. Introduction. Lipid oxidation products and atherosclerosis. *Vascul. Pharmacol*. 38, 187-191, 2002.

6 Bhaskaran S, Santanam N, Penumetcha M, and Parthasarathy S. Inhibition of atherosclerosis in low-density lipoprotein receptornegative mice by sesame oil. *J Med Food* 9:487–490, 2006.

7 Budoff JM and Gul KM. Expert review on coronary calcium. *Vasc Health Risk Manag*. 4(2): 315–324, 2008.

8 Cardús A, Panizo S, Parisi E, Fernandez E, and Valdivielso JM. Differential effects of vitamin D analogs on vascular calcification. *J Bone Miner Res*. 22(6):860-866, 2007.

9 Chandrakala AN, Selvarajan K, Burge KY, Litvinov D, Sengupta B and Parthasarathy S. Water-soluble Components of Sesame Oil reduce inflammation and atherosclerosis. *Journal of Medicinal Food*. 19(7):1-9, 2016.

10 Chandrakala AN, Selvarajan K, Litvinov D, Parthasarathy S. Anti-Atherosclerotic and Anti-Inflammatory Actions of Sesame Oil. *Journal of Medicinal Food*. 205;18(1):11-20, 2015.

11 Demer LL and Tintut Y. Vascular Calcification Pathobiology of a Multifaceted Disease. *Circulation*. 104(16): 1881–1883, 2001.

12 Dhore CR, Cleutjens JP, Lutgens E, Cleutjens KB, Geusens PP, Kitslaar PJ, Tordoir JH, Spronk HM, Vermeer C, and Daemen MJ.Differential expression of bone matrix regulatory proteins in human atherosclerotic plaques. *Arterioscler Thromb Vasc Biol* 21: 1998–2003,

2001.

13 Doyle IR, Ryall RL, and Marshall VR. Inclusion of proteins into calcium oxalate crystals precipitated from human urine: a highly selective phenomenon. *Clin. Chem* 37:1589–1594, 1991.

14 Eggen DA, Strong JP, and McGill HC. Coronary calcification: relationship to clinically significant coronary lesions and race, sex and topographic distribution. *Circulation*. 32:948–955, 1965.

15 Elewski B, and Thiboutot D. A clinical overview of azelaic acid. *Cutis* 77:12–16, 2006.

16 Esterbauer H, Koller E, Slee RG, and Koster JF. Possible involvement of the lipid-peroxidation product 4-hydroxynonenal in the formation of fluorescent chromolipids. *Biochem J.* 239:405–409,1986.

17 Fruebis J, Parthasarathy S, and Stienberg D. Evidence for a concerted reaction between lipid hydroperoxides and polypeptides. *Proc. Nati. Acad. Sci. USA*. 89: 10588-10592, 1992.

18 Godfraind T, Sturbois X, and Verbeke N. Calcium incorporation by smooth muscle microsomes. *Biochim. Biophys. Acta* 455:254–268, 1976.

19 Gooderham M. Rosacea and its topical management. *Skin Therapy Lett.* 14:1–3, 2009.

20 Hayden MR, Tyagi SC, Kolb L, Sowers JR, and Khanna R. Vascular ossification – calcification in metabolic syndrome, type 2 diabetes mellitus, chronic kidney disease, and calciphylaxis – calcific uremic arteriolopathy: the emerging role of sodium thiosulfate. *Cardiovascular Diabetology* 4:4, 2005.

21 Iraji F, Sadeghinia A, Shahmoradi Z, Siadat AH, and Jooya A. Efficacy of topical azelaic acid gel in thetreatment of mild-moderate acne vulgaris. *Indian J. Dermatol. Venereol. Leprol* 73:94–96, 2007.

22 Jessup W, Jurgens G, Lang J, Esterbauer H, and Dean RT. Interaction of 4-hydroxynonenal-modified low-density lipoproteins with the fibroblast apolipoprotein B/E receptor. *Biochem J.* 234:245–248, 1986.

23 Johnson RC, Leopold JA, and Loscalzo J. Vascular calcification: pathobiological mechanisms and clinical implications. *Circ Res*. 99:1044–1059, 2006.

24 Jono S, Nishizawa Y, Shioi A, and Morii H. 1,25-Dihydroxyvitamin D3 increases in vitro vascular calcification by modulating secretion of endogenous parathyroid hormone-related peptide. *Circulation*. 98(13):1302-1306, 1998.

25 Jürgens G, Lang J, and Esterbauer H. Modification of human low-density lipoprotein by the lipid peroxidation product 4-hydroxynonenal. *Biochim. Biophys. Acta*. 875:103–114, 1986.

26 Kaneko T, Kaji K, and Matsuo M. Cytotoxicities of a linoleic acid hydroperoxide and its related aliphatic aldehydes toward cultured human umbilical vein endothelial cells. *Chem Biol Interact*, 67(3-4): 295-304,1988.

27 Kamido H, Eguchi H, Ikeda H, Imaizumi T, Yamana K, Hartvigsen K, Ravandi A, and Kuksis A. Core aldehydes of alkyl glycerophosphocholines in atheroma induce platelet aggregation and inhibit endothelium-dependent arterial relaxation. *J. Lipid Res*. 43:158–166, 2002.

28 Li WG, Stoll LL, Rice JB, Xu SP, Miller FJ Jr, Chatterjee P, Hu L, Oberley LW, Spector AA, and Weintraub NL. Activation of NAD(P)H oxidase by lipid hydroperoxides: mechanism of oxidant-mediated smooth muscle cytotoxicity. *Free Radic Biol Med.* 34(7):937-46, 2003.

29 Litvinov D, Selvarajan K, Garelnabi M, Brophy L, and Parthasarathy S. Anti-atherosclerotic actions of azelaic acid, an end product of linoleic acid peroxidation, in mice. *Atherosclerosis* 209:449-454, 2010.

30 Lopez MA, Vicente J, Kulasekaran S, Vellosillo T, Martínez M, Irigoyen ML, Cascón T, Bannenberg G, Hamberg M, Castresana C. Antagonistic role of 9-lipoxygenase-derived oxylipins and ethylene in the control of oxidative stress, lipid peroxidation and plant defence. *Plant J*, 67(3): 447-58, 2011.

31 Mackey RH, Venkitachalam L, and Sutton-Tyrrell K. Calcifications, arterial stiffness and atherosclerosis. *Adv. Cardiol* . 44:234–244, 2007.

32 Marathe GK, Davies SS, Harrison KA, Silva AR, Murphy RC, Castro-Faria-Neto H,. Prescott SM, Zimmerman GA, and McIntyre TM. Inflammatory platelet-activating factor-like phospholipids in oxidized low density lipoproteins are fragmented alkyl phosphatidylcholines. *J. Biol. Chem.* 274: 28395–28404,1999.

33 Marchi I, Viette V, Badoud F, Fathi M, Saugy M, Rudaz S, Veuthey J. Characterization and classification of matrix effects in biological samples analyses. *Journal of Chromatography*,

Antioxidants and Redox Signaling
A novel mechanism for atherosclerotic calcification-potential resolution of the oxidation paradox. (DOI: 10.1089/ars.2017.7362)
This paper has been peer-reviewed and accepted for publication, but has yet to undergo copyediting and proof correction. The final published version may differ from this proof.

1217:4071–4078, 2010.

34 Mazzini MJ, and Schulze PC. Proatherogenic pathways leading to vascular calcification. *Eur. J. Radiol* 57:384–389, 2006.

35 Mizobuchi M, Finch JL, Martin DR, and Slatopolsky E. Differential effects of vitamin D receptor activators on vascular calcification in uremic rats. *Kidney Int.* 72(6):709-715, 2007.

36 Nicoll R, Henein MY. The predictive value of arterial and valvular calcification for mortality and cardiovascular events. *IJC Heart & Vessels* 3: 1-5, 2014.

37 O'Toole TE, Zheng YT, Hellmann J, Conklin DJ, Barski O, and Bhatnagar A. Acrolein activates matrix metalloproteinases by increasing reactive oxygen species in macrophages. *Toxicol Appl Pharmacol*. 236(2): 194–201, 2009.

38 Parthasarathy S, Merchant NK, Penumetcha M, and Santanm N: Oxidation and cardiovascular disease-potential role of oxidants in inducing antioxidant defense enzymes. *J Nucl Cardiol* 8:379-389, 2001.

39 Parthasarathy S, Santanam N, Ramachandran S, and Meilhac O. Oxidants and antioxidants in atherogenesis: an appraisal. *J Lip Res*. 40: 2143-2157, 1999.

40 Parthasarathy S, Steinbrecher P, Barnett J, Witztum JL, and Steinberg D. Essential role of phospholipase A2 activity in endothelial cell induced modification of low density lipoprotein. Proc. Natl. Acad. Sci. USA 82:3000-3004, 1985.

41 Parthasarathy S. Modified Lipoproteins in the Pathogenesis of Atherosclerosis. R. G. Landes Co. Austin, TX. 1994.

42 Qi YF, Wang SH, Zhang BH, Bu DF, Shu TC, and Du JB. Changes in amount of ADM mRNA and RAMP2 mRNA in calcified vascular smooth muscle cells. *Peptides*. 24(2):287-294, 2003.

43 Quehenberger O, Koller E, Jürgens G, and Esterbauer H. Investigation of lipid peroxidation in human low density lipoprotein. *Free. Radic. Res. Commun*. 3:233–242, 1987.

44 Quinn MT, Parthasarathy S and Steinberg D. Lysophosphatidylcholine: A chemotactic factor for human monocytes and its potential role in atherogenesis. *Proc. Natl. Acad. Sci. USA* 85: 2805-2809, 1988.

45 Raghavamenon A, Garelnabi M, Babu S, Aldrich A, Litvinov D, and Parthasarathy S. Alpha-tocopherol is ineffective in preventing the decomposition of preformed lipid peroxides and may promote the accumulation of toxic aldehydes: a potential explanation for the failure of antioxidants to affect human atherosclerosis. *Antioxid Redox Signal.* 11(6):1237-1248, 2009.

46 Requena JR, Fu MX, Ahmed MU, Jenkins AJ, Lyons TJ, Baynes JW, and Thorpe SR. Quantification of malondialdehyde and 4- hydroxynonenal adducts to lysine residues in native and oxidized human low-density lipoprotein. Biochem. J 322:317–325, 1997.

47 Rong R, Ramachandran S, Penumetcha M, Khan N, Parthasarathy S. Dietary oxidized fatty acids may enhance intestinal apolipoprotein A-I production. *J Lipid Res*, 43(4): 557-564. 2002.

48 Ross R. Atherosclerosis--an inflammatory disease. *N. Engl. J. Medicine*. 340:115–126, 1999.

49 Shih DM, Xia Y, Wang X, Milleri E, Castellani LW, Subbanagounder G, Cheroutre H, Faull KF, Berliner JA, Witztumi JL, and Lusis AJ. Combined Serum Paraoxonase Knockout/Apolipoprotein E Knockout Mice Exhibit Increased Lipoprotein Oxidation and Atherosclerosis. The Journal of Biological Chemistry 275 (23):17527–17535, 2000.

50 Sigruener A, Buechler C, Orsó E, Hartmann A, Wild PJ, Terracciano L, Roncalli M, Bornstein SR, and Schmitz G. Human aldehyde oxidase 1 interacts with ATP-binding cassette transporter-1 and modulates its activity in hepatocytes. *Horm Metab Res*. 39(11):781-789, 2007.

51 Spiteller G. Linoleic acid peroxidation--the dominant lipid peroxidation process in low density lipoprotein--and its relationship to chronic diseases. *Chem.Phys. Lipids* 95:105–162, 1998.

52 Stary H, Chandler A, Glagov S, Guyton J, Insull W, Jr, Rosenfeld M, Schaffer SA, Schwartz CJ, Wagner WD, and Wissler RW. A definition of initial, fatty streak, and intermediate lesions of atherosclerosis. A report from the Committee on Vascular Lesions of the Council on Arteriosclerosis, American Heart Association. *Arterioscler. Thromb*. 14:840–856, 1994.

53 Stary HC. Natural history of calcium deposits in atherosclerosis progression and regression. *Z Kardiol* 89:28–35. 2000.

54 Steinberg D, Parthasarathy S, Crew TE, Khoo JC, and Witztum JL. Beyond cholesterol: modification of low-density lipoprotein that increase its atherogenecity. *N. Engl. J. Med.* 320: 915–924, 1989.

55 Steinberg D. Oxidative Modification of LDL and Atherogenesis. Circulation. 95:1062-1071, 1997.

56 Tamar SP, McClelland RL, Jorgensen NW, Bild D, Burke GL, Guerci AD and Greenland P. Coronary Artery Calcium Score and Risk Classification for Coronary Heart Disease Prediction: The Multi-Ethnic Study of Atherosclerosis. *JAMA*. 303(16): 1610–1616, 2010.

57 Vengrenyuk Y, Carlier S, Xanthos S, Cardoso L, Ganatos P, Virmani R, Einav S, Gilchrist L, and Weinbaum S. A hypothesis for vulnerable plaque rupture due to stress-induced debonding around cellular microcalcifications in thin fibrous caps. *Proc. Natl. Acad. Sci. U S A*. 103:14678–14683, 2006.

58 Virmani R, Burke AP, Farb A, and Kolodgie FD. Pathology of the vulnerable plaque. *J. Am. Coll. Cardiol*. 47:c13–c18, 2006.

59 Young SG, and Parthasarathy S. Why Are Low-Density Lipoproteins Atherogenic? *WJM*, 160(2):153-164, 1994.

Antioxidants and Redox Signaling
A novel mechanism for atherosclerotic calcification-potential resolution of the oxidation paradox. (DOI: 10.1089/ars.2017.7362)
This paper has been peer-reviewed and accepted for publication, but has yet to undergo copyediting and proof correction. The final published version may differ from this proof.

Abbreviations

4-HNE	4-Hydroxy nonenal
ALP	Alkaline phosphatase
AOX	Aldehyde oxidase
AP	ApoE-PON1
ApoE	Apolipoprotein E
AzA	Azelaic acid
Ca	Calcium
Ca-AzA	Calcium azelate
CHD	Coronary heart disease
CT	Computerized tomography
DCA	Dicarboxylic acids
DKO	Double knockout
EDTA	Ethylenediaminetetraacetic acid
ESI	Electrospray ionization
HASMC	Human aortic smooth muscle cells
HPODE	13-Hydroperoxyoctadecadienoic acid
IS	Internal standard
LC-MS	Liquid chromatography-Mass spectrometry
LDL	Low density lipoprotein
LOD	Limit of detection
LOQ	Limit of quantification
Na	Sodium
Na-AzA	Sodium azelate

MPO	Myeloperoxidase
ONA	9-Oxononanoic acid
Ox-LDL	Oxidized LDL
PON1	Paraoxonase 1
PtdCho	Phosphatidylcholine
PUFA	Poly-unstaturated fatty acid
QTOF-MS	Quadrupole time of flight mass spectrometer
Vit E	Vitamin E

Antioxidants and Redox Signaling
A novel mechanism for atherosclerotic calcification-potential resolution of the oxidation paradox. (DOI: 10.1089/ars.2017.7362)
This paper has been peer-reviewed and accepted for publication, but has yet to undergo copyediting and proof correction. The final published version may differ from this proof.

Figure Legends

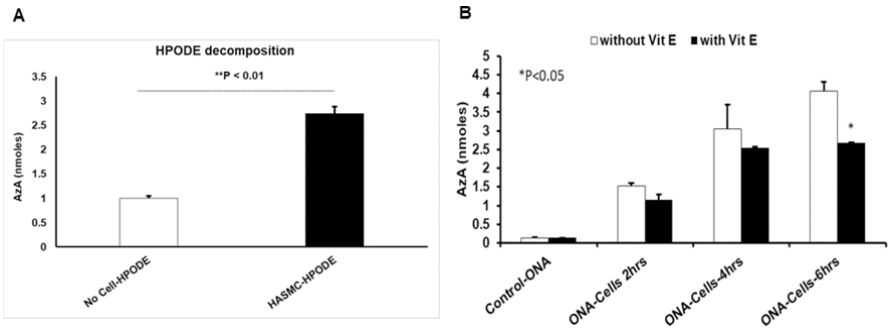

Figure 1: HASMC induced decomposition of HPODE and Conversion of ONA to AzA is inhibited by α-Tocopherol. HASMCs were grown to confluence and incubated with A) HPODE and B) ONA in the presence and absence of α-tocopherol for 6 hrs. After treatment, AzA was quantified by LC-MS analysis.

Antioxidants and Redox Signaling
A novel mechanism for atherosclerotic calcification-potential resolution of the oxidation paradox. (DOI: 10.1089/ars.2017.7362)
This paper has been peer-reviewed and accepted for publication, but has yet to undergo copyediting and proof correction. The final published version may differ from this proof.

Antioxidants and Redox Signaling
A novel mechanism for atherosclerotic calcification-potential resolution of the oxidation paradox. (DOI: 10.1089/ars.2017.7362)

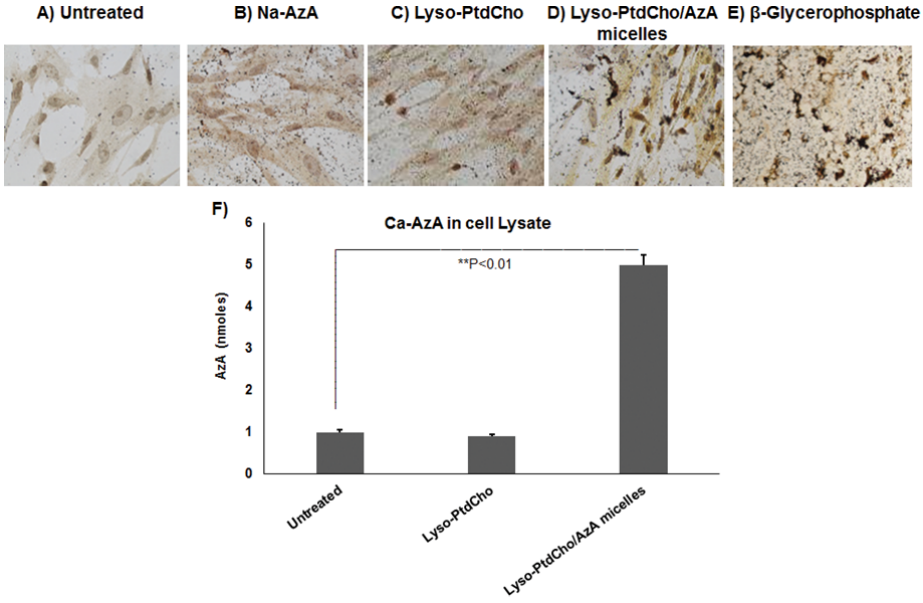

Figure 2. Calcification of HASMC induced by AzA micelle treatment. Cells were grown to confluence and incubated for 9 days under the following conditions: A. Untreated B. Na-AzA at 100µmole per liter C. Lyso-PtdCho micelles at 50 µmole per liter D. Lyso-PtdCho/AzA Micelles at 50 µmole per liter / 100 µmole per liter. E. 10 mmoles per liter β-glycerophosphate. Cells were stained for calcium deposits using von Kossa staining (calcium deposits appear dark brown spots). Image Magnification 40X. F. AzA quantification in nmoles of calcium deposit associated AzA

Antioxidants and Redox Signaling
A novel mechanism for atherosclerotic calcification-potential resolution of the oxidation paradox. (DOI: 10.1089/ars.2017.7362)

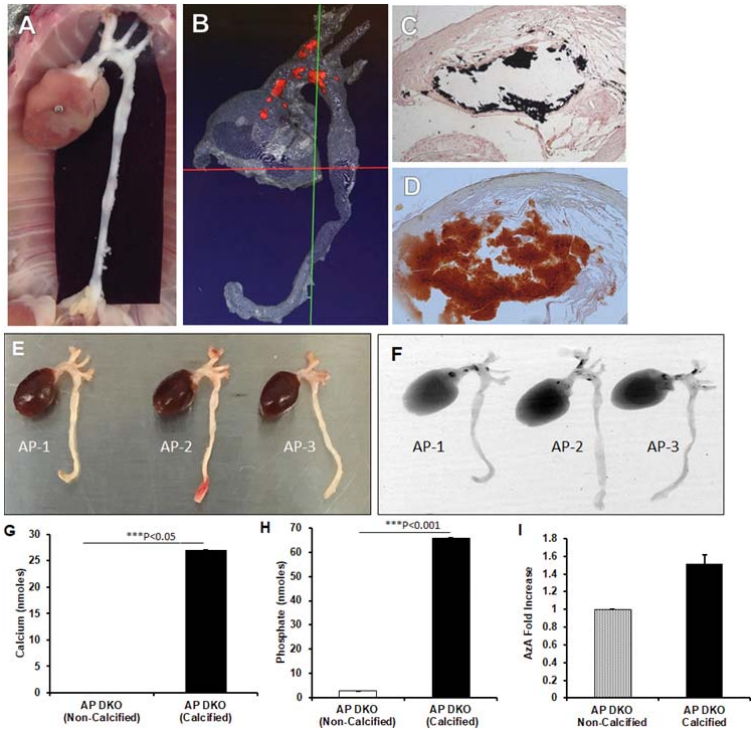

Figure 3. Calcification in aged ApoE-PON1 double knockout mice. A. Photograph of dissected aortic loop. B. microCT scan of dissected aortic loop C. Calcium stain of aortic loop cross sections (image magnification 10x) stained with B. von Kossa stain and D. Alizarin Red S stain. E. Images of dissected mouse aorta. F. X-ray scan image of dissected mouse aorta. G. Calcium quantification of mouse lesion calcified domains. H. Phosphate quantification of mouse lesion calcified domains. I. Fold increase in LC-MS signal for AzA in mouse calcified domains. Mean±SEM, * $p \leq 0.05$, ** $p \leq 0.01$, *** $p \leq 0.001$, (t-test).

Antioxidants and Redox Signaling
A novel mechanism for atherosclerotic calcification-potential resolution of the oxidation paradox. (DOI: 10.1089/ars.2017.7362)

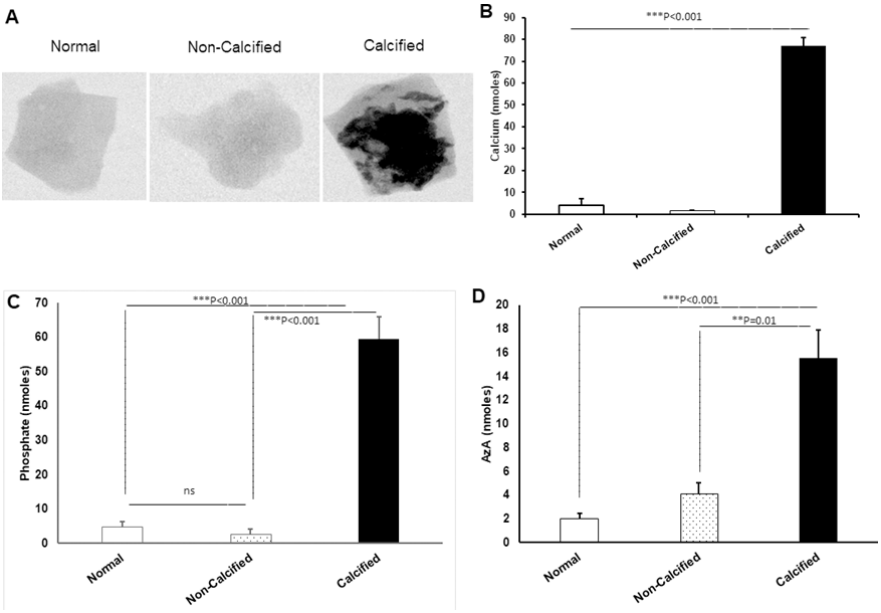

Figure 4. Calcification in human aortic tissue samples A. X-ray images showing calcified regions as dark regions. B. Calcium quantification of calcium deposit associated calcium. C. Phosphate quantification in nmoles of calcium deposit associated phosphate. D. AzA quantification in nmoles of calcium deposit associated AzA. Mean±SEM, n=9, * $p \leq 0.05$, ** $p \leq 0.01$, *** $p \leq 0.001$ (One way ANOVA Bonferroni multiple comparison test)

Antioxidants and Redox Signaling
A novel mechanism for atherosclerotic calcification-potential resolution of the oxidation paradox. (DOI: 10.1089/ars.2017.7362)

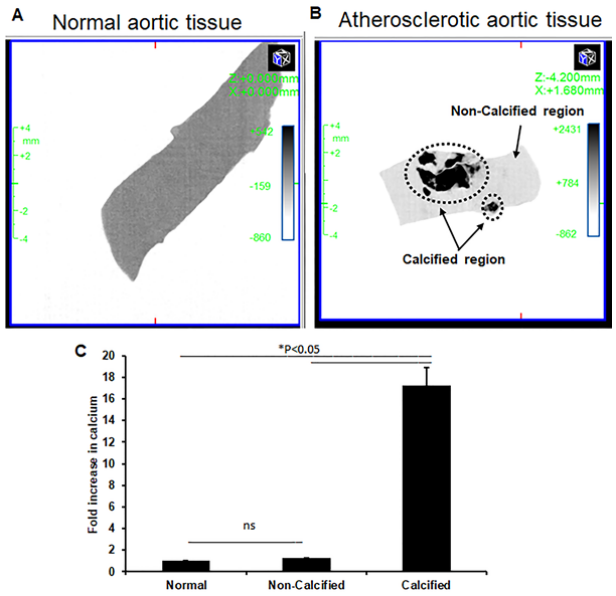

Figure 5. Human aortic tissue microCT images. A. Representative cross sections of microCT images for human aortic tissue samples. B. Densitometry of calcified domains. Mean±SEM, * $p \leq 0.05$, ** $p \leq 0.01$, *** $p \leq 0.001$(t-test).

Antioxidants and Redox Signaling
A novel mechanism for atherosclerotic calcification-potential resolution of the oxidation paradox. (DOI: 10.1089/ars.2017.7362)

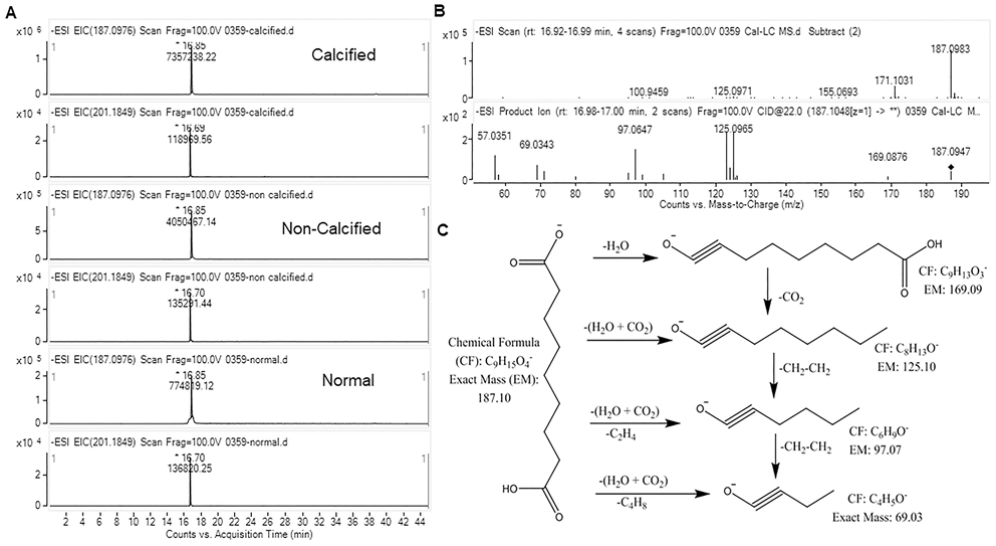

Figure 6: The representative LC-ESI-HRMS extracted ion chromatograms - AzA ($[M-H]^-$ 187.0976) and AzA-D14 (IS, ($[M-H]^-$ 201.1849)) (A), ESI-MS and MS/MS spectra (B) and proposed fragment ions (C).

Antioxidants and Redox Signaling
A novel mechanism for atherosclerotic calcification-potential resolution of the oxidation paradox. (DOI: 10.1089/ars.2017.7362)

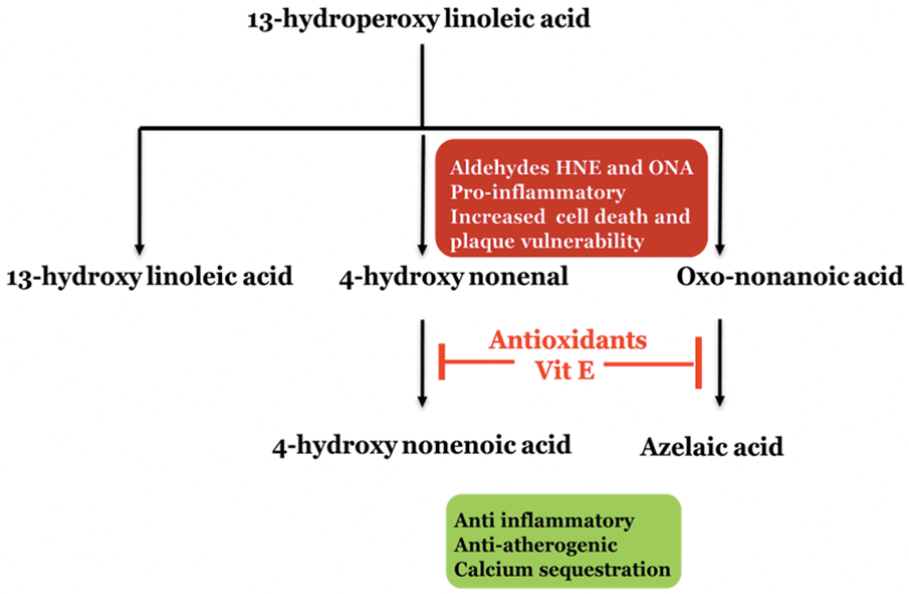

Figure 7: Schematic representation of the hypothesis.

Supplementary Table 1. Human Aortic Tissue Samples Clinical Diagnosis of Subjects.

Sample Number	Gender	Age	Clinical Diagnosis	Diagnosis Report
1	M	68	Chronic Systolic Heart Failure, Stroke, Severe Calcific Atherosclerosis of (Thoracic and Abdominal Aorta, Left Main Coronary, Right Coronary, and Left Circumflex Arteries), Moderate to Severe calcific Atherosclerosis (Left Anterior Descending Artery)	Atherosclerosis
2	M	71	Acute Pancreatitis, Hypertriglyceridemia, Coronary Artery disease, Hypertension, Diabetes Mellitus Type 2, Abdominal aortic Aneurysm, Obstructive Sleep Apnea, Gout	
3	M	71	Coronary Artery Disease (Vessel Bypass Grafting), Myocardial Infarction with Subsequent Stenting, Severe Aortic Stenosis, Paroxysmal Atrial Fibrillation, Hypertension, Dyslipidemia, Nhypothyroidism, Benign Prostatic Hypertrophy, Obstructive Sleep Apnea, Obesity, Tobacco Abuse, History of DVT	Atherosclerosis
4	M	73	Atherosclerosis, deep venous thrombisis	Atherosclerosis
5	M	51	End Stage Renal Disease (Failed Surgery), Diabetes Mellitus Type I, Hypertension, Hyperlipidemia, Atherosclerosis	
6	M	62	Atherosclerosis	Atherosclerosis
7	M	87	Pneumonia, Chronic Hypoxic Hypercapenic Respiratory Failure, Acute Kidney Insufficiency, Chronic Obstructive Pulmonary Disease, B-Cell Lymphoma (in Remission), Coronary Artery Disease, Heart Failure	Atherosclerosis
8	M	67	Atrial Fibrillation, Chronic Hypertensions, Acute Pulmonary Embolism, Chronic Obstructive Pulmonary Disease, Respiratory failure with Hypoxia, Obesity (BMI 34), Diabetes Mellitus Type 2, Diabetic neuropathy, Anemia, Chronic Gastroesophageal Reflux Disease, Gouty arthritis	Atherosclerosis
9	M	64	Hypertension, kidney stones, gout, high cholesterol, benign prostatic hyperplasia.	

Antioxidants and Redox Signaling
A novel mechanism for atherosclerotic calcification-potential resolution of the oxidation paradox. (DOI: 10.1089/ars.2017.7362)

Supplementary Table 3. Human Aortic Tissue Samples Quantified Molecules in nmoles.

	Normal tissue			Non-Calcified Atherosclerotic Tissue			Calcified Atherosclerotic Tissue		
Sample	AzA (nmoles)	Calcium (nmoles)	Phosphate (nmoles)	AzA (nmoles)	Calcium (nmoles)	Phosphate (nmoles)	AzA (nmoles)	Calcium (nmoles)	Phosphate (nmoles)
1	1.03	ND	3.648	8.46	ND	ND	18.22	68.6	36.779
2	4.92	2.41	5.559	0.48	ND	ND	19.68	82.7	76.463
3	0.6	0.27	5.101	6.24	ND	1.882	21.49	90.5	87.363
4	1.24	ND	2.305	1.95	ND	6.858	17.47	58.7	39.923
5	0.78	10.12	11.863	3.04	1.64	1.06	11.01	77.9	59.875
6	1.37	ND	0.599	3.31	ND	1.107	27.72	88.4	70.697
7	1.41	ND	ND	1.85	ND	ND	6.71	78.13	59.686
8	2.65	ND	ND	6.85	ND	ND	9.25	71.88	44.472
9	3.86	ND	ND	4.9	ND	ND	8.07	ND	ND
Average	1.984	4.267	4.846	4.12	1.64	2.727	15.513	77.101	59.407
SEM	0.502	1.727	1.297	0.884	0.1	0.927	2.374	3.515	6.062

Antioxidants and Redox Signaling
A novel mechanism for atherosclerotic calcification-potential resolution of the oxidation paradox. (DOI: 10.1089/ars.2017.7362)

Supplementary Figure Legends

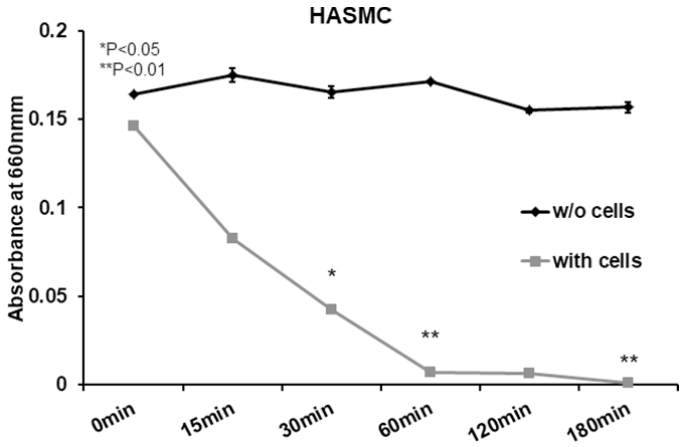

Supplementary Figure 1. Decomposition of HPODE by HASMC. HASMC were incubated with 100 µmoles/L HPODE. Decomposition of peroxides was determined by LMB assay over time both in the presence and absence of cells. Mean±SEM, n=3; * $p \leq 0.05$, ** $p \leq 0.01$ (t-test)

Antioxidants and Redox Signaling
A novel mechanism for atherosclerotic calcification-potential resolution of the oxidation paradox. (DOI: 10.1089/ars.2017.7362)

Antioxidants and Redox Signaling
A novel mechanism for atherosclerotic calcification-potential resolution of the oxidation paradox. (DOI: 10.1089/ars.2017.7362)

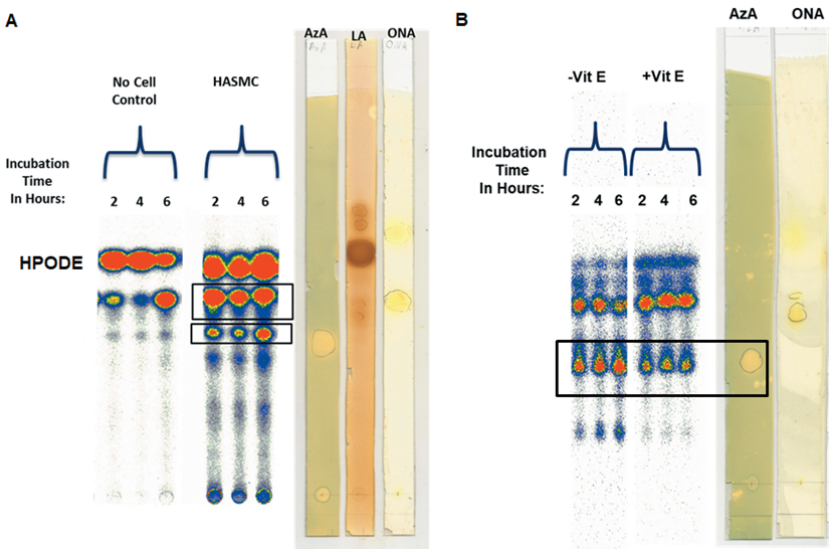

Supplementary Fig 2: Thin Layer Chromatography autoradiograph of the lipid fraction from A. HPODE decomposition products, both in presence and absence of HASMC cells in medium over time, and B. Conversion of ONA to AzA by HASMC in presence and absence of (Vit E) α-tocopherol. Representative images of three independent experiments.

Antioxidants and Redox Signaling
A novel mechanism for atherosclerotic calcification-potential resolution of the oxidation paradox. (DOI: 10.1089/ars.2017.7362)

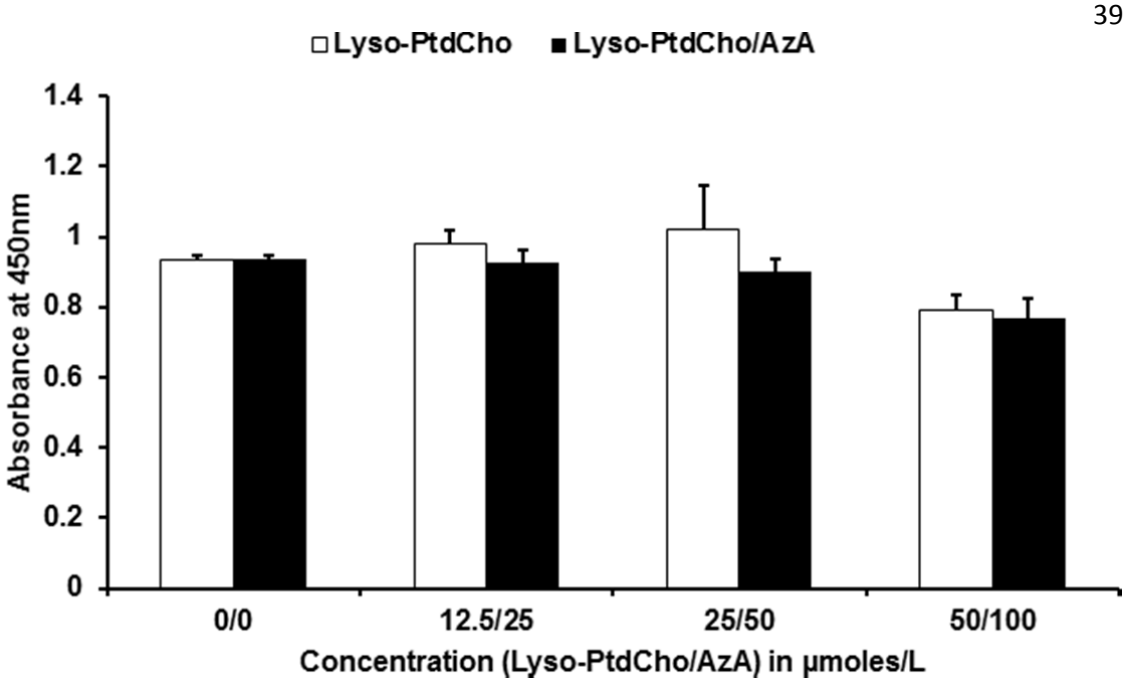

Supplementary Figure 3. The effect of Lyso-PtdCho/AzA micelle treatment on HASMC cell viability. HASMC were exposed to Lyso-PtdCho micelles at concentration 50 µmole per liter and Lyso-PtdCho/AzA at 50 µmole per liter / 100 µmole per liter, and the WST-1 assay was performed following the instructions of suppliers protocol. Viable cells metabolize WST-1 reagent increasing the absorbance at 450nm. Mean±SEM, n=3; Untreated vs Treated, * $p \leq 0.05$, ** $p \leq 0.01$ (t-test)

Antioxidants and Redox Signaling
A novel mechanism for atherosclerotic calcification-potential resolution of the oxidation paradox. (DOI: 10.1089/ars.2017.7362)

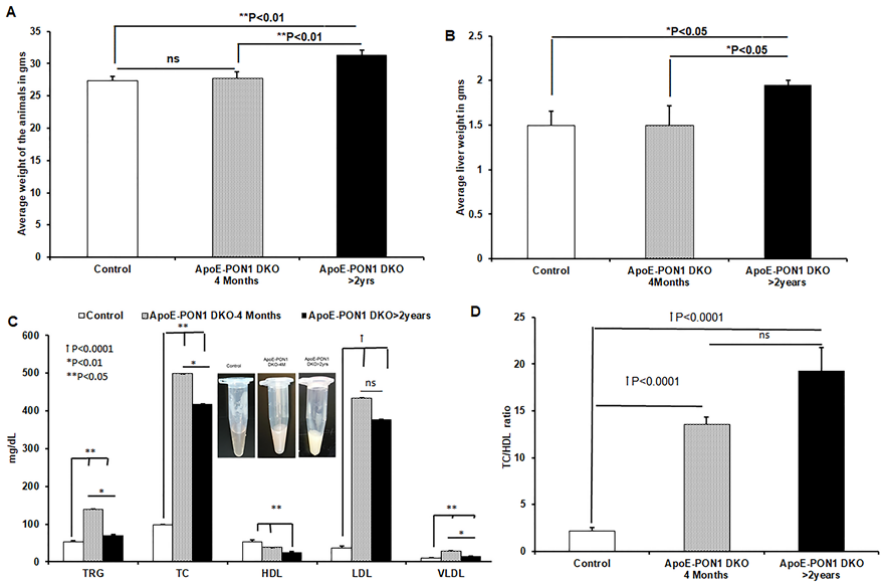

Supplementary Figure 4. ApoE-Pon1 DKO Plasma Lipids Profile. Young (4 month) and aged (≥2 year) DKO mice were compared with control mice. A. Average weight of mice in grams. B. Average liver weight of mice in grams. C. Lipid profile of mice (in mg/DL) of triglycerides, total cholesterol, high density lipoprotein, low density lipoprotein, and very low density lipoprotein. D. Ratio of Total Cholesterol to HDL. Mean±SEM; Untreated vs Treated, * $p \leq 0.05$, ** $p \leq 0.01$, (t-test)

Antioxidants and Redox Signaling
A novel mechanism for atherosclerotic calcification-potential resolution of the oxidation paradox. (DOI: 10.1089/ars.2017.7362)

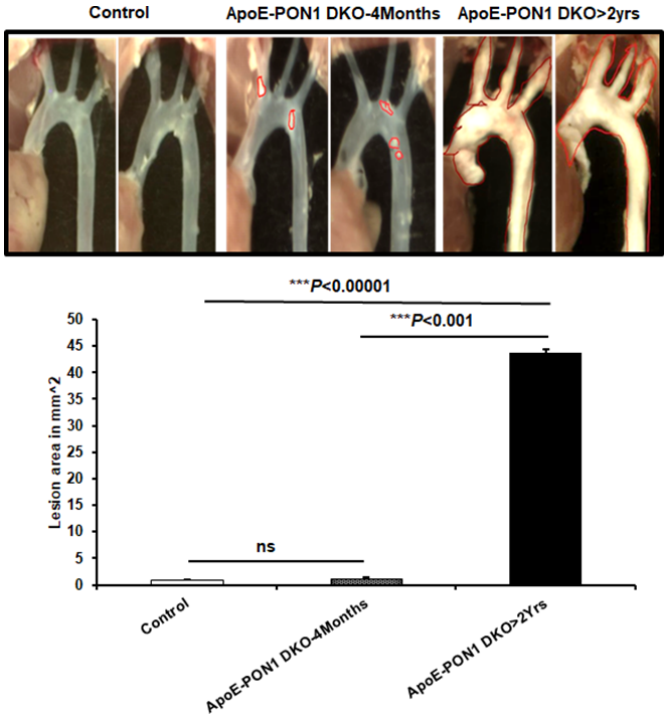

Supplementary Figure 5. Lesion area of ApoE-Pon1 DKO mice. A. Photographs of lesion areas in dissected aortic loops. B. Quantified lesion area of mice in mm^2. Mean±SEM;, *** $p \leq 0.001$.